Biochimica et Biophysica Acta 1843 (2014) 2926–2936

Contents lists available at ScienceDirect

Biochimica et Biophysica Acta

journal homepage: www.elsevier.com/locate/bbamcr

Mitochondrial pro-apoptotic indices do not precede the transient caspase activation associated with myogenesis

Darin Bloemberg, Joe Quadrilatero *

University of Waterloo, Waterloo, Ontario, Canada

ARTICLE INFO

Article history:
Received 30 May 2014
Received in revised form 18 August 2014
Accepted 2 September 2014
Available online 7 September 2014

Keywords:
Skeletal muscle
Differentiation
Apoptosis
Mitochondrion
Cytochrome c
XIAP

ABSTRACT

Skeletal muscle differentiation requires activity of the apoptotic protease caspase-3. We attempted to identify the source of caspase activation in differentiating C2C12 skeletal myoblasts. In addition to caspase-3, caspase-2 was transiently activated during differentiation; however, no changes were observed in caspase-8 or -9 activity. Although mitochondrial Bax increased, this was matched by Bcl-2, resulting in no change to the mitochondrial Bax:Bcl-2 ratio early during differentiation. Interestingly, mitochondrial membrane potential increased on a timeline similar to caspase activation and was accompanied by an immediate, temporary reduction in cytosolic Smac and cytochrome c. Since XIAP protein expression dramatically declined during myogenesis, we investigated whether this contributes to caspase-3 activation. Despite reducing caspase-3 activity by up to 57%, differentiation was unaffected in cells overexpressing normal or E3-mutant XIAP. Furthermore, a XIAP mutant which can inhibit caspase-9 but not caspase-3 did not reduce caspase-3 activity or affect differentiation. Administering a chemical caspase-3 inhibitor demonstrated that complete enzyme inhibition was required to impair myogenesis. These results suggest that neither mitochondrial apoptotic signaling nor XIAP degradation is responsible for transient caspase-3 activation during C2C12 differentiation.

1. Introduction

Apoptosis is a tightly controlled physiological process that typically results in the removal of abnormal, damaged, and/or unnecessary cells [1]. Upstream apoptotic events converge on a set of proteolytic enzymes known as caspases, which cleave various proteins leading to DNA damage and cell disassembly. Caspases become activated in response to the binding of extracellular death ligands, and as a result of intracellular stressors sensed by the mitochondria and endoplasmic reticulum [2–5]. Cells possess a number of anti-apoptotic capabilities, and this balance between pro- and anti-apoptotic signaling determines the extent of caspase activation and ultimately cell death [1]. During development, apoptosis is responsible for shaping tissues by eliminating cells deemed unnecessary. However, evidence suggests that apoptotic signaling contributes to differentiation in several cell types including some epithelial tissues, erythrocytes, and skeletal muscle [6].

Skeletal muscle differentiation occurs during embryonic development whereby a population of single-nucleated stem cell-like myoblasts exit cell cycle and fuse to form multinucleated myotubes. This process is controlled by a number of hormones, cell cycle regulators, specific inhibitor of differentiation (Id) proteins, and transcription factors (i.e. MyoD, Myf-5, MRF-4, and myogenin) known as myogenic regulatory factors (MRFs) [7,8]. As with other tissue types, widespread cell death occurs in skeletal muscle during development. Interestingly, MyoD has been shown to regulate apoptotic signaling in cells that die during the differentiation process [9,10]. Furthermore, several phenotypic alterations typical of apoptosis also occur in surviving cells during myogenesis. This includes cytoskeletal reorganization [11], activation of matrix metalloproteinases [12], and the extracellular exposure of phosphatidylserine [13].

In fact, previous studies have shown that caspase activation, particularly caspase-3, is required for skeletal muscle formation [14]. In this seminal paper, primary myoblasts taken from caspase-3 null mice did not form myotubes or express markers of differentiation [15]. Furthermore, a caspase-3 substrate, MST1, was shown to be cleaved, and the provision of its active product partially restored differentiation in caspase-3 null cells [15]. Since then, other pro-differentiation caspase targets have been identified. This includes the bHLH transcription factor Twist, which inhibits MyoD and MEF2 [16,17], the MEF2 repressor HIPK2 [18], and the typically pro-apoptotic target CAD, which is necessary for proper induction of p21 [19].

Aside from substrate specificity, it has been suggested that the manner of caspase activation determines the "die or differentiate" decision [14]. Caspase activity during differentiation occurs transiently and reportedly at a lower intensity than during apoptosis [14,15,20]. Therefore, it may be this fine-tuning of apoptotic signaling that allows surviving cells to avoid death and instead progress through the

* Corresponding author at: Department of Kinesiology, University of Waterloo, 200 University Ave. West, Waterloo, Ontario N2L3G1, Canada. Tel.: +1 519 888 4567; fax: +1 519 885 0470.
E-mail address: jquadril@uwaterloo.ca (J. Quadrilatero).

http://dx.doi.org/10.1016/j.bbamcr.2014.09.002
0167-4889/

myogenic program. It is currently unknown, however, how caspase-3 becomes active in differentiating cells, and how this signaling is maintained transiently. Previous studies have implicated the involvement of typical apoptotic mechanisms such as Bcl-xL/caspase-9 [20] and FADD/caspase-8 [21]. However, specific hallmarks such as mitochondrial permeabilization and release of pro-apoptotic factors have not been shown in differentiating myoblasts.

Therefore, the purpose of this study was to assess typical apoptosis signaling in differentiating skeletal muscle cells to identify the relevant source of caspase activation. Based on initial observations, we further examined the role XIAP may play in this context.

2. Materials and methods

2.1. Cell culture

C2C12 mouse skeletal myoblasts (ATCC) were cultured in growth media (GM) consisting of low-glucose Dulbecco's Modified Eagle's Medium (DMEM; Hyclone, ThermoFisher) containing 10% fetal bovine serum (FBS; ThermoFisher) and 1% penicillin/streptomycin (ThermoFisher) on polystyrene cell culture dishes (BD Biosciences). Upon reaching 80–90% confluence, differentiation was induced by replacing GM with differentiation media (DM) consisting of DMEM supplemented with 2% horse serum (Hyclone, ThermoFisher) and 1% penicillin/streptomycin. Cells were isolated and utilized for various biochemical analyses immediately prior to the induction of differentiation (day 0), and at several subsequent time points. In some experiments C2C12 cells were treated with staurosporine (2 μM, Enzo Life Sciences), oligomycin (2.5 μM or 10 μM, Cayman Chemical), or the caspase-3 inhibitor Ac-DEVD-CHO (5 μM, 10 μM, or 30 μM, Enzo Life Sciences).

2.2. Isolation and subcellular fractionation

In order to avoid the potential effects of apoptotic events happening in cells which die during differentiation, cells in culture were always washed three times with warmed PBS before being removed for analyses. After washing, cells were isolated via trypsinization and centrifuged at 1000 *g*. Whole-cell lysates were generated by adding lysis buffer (LB, pH 7.4; 20 mM HEPES, 10 mM NaCl, 1.5 mM MgCl, 1 mM DTT, 20% glycerol, and 0.1% Triton-X100, Sigma Aldrich) with protease inhibitors (Complete Cocktail; Roche) followed by sonication for 20 s.

Additional cells were separated into cytosolic-, mitochondrial-, and nuclear-enriched fractions [22,23]. After trypsinization and washing, cells were incubated in digitonin buffer (PBS with 250 mM sucrose, 80 mM KCl, and 50 μg/mL digitonin, Sigma Aldrich) for 5 min on ice. Cells were centrifuged at 1000 *g* for 10 min, the supernatant was collected and centrifuged at 16,000 *g* for 10 min to pellet any mitochondrial contamination, and the supernatant from this spin was kept as the cytosolic-enriched fraction. The pellet (P1) remaining from the 1000 g spin was washed in PBS, centrifuged at 1000 *g* for 5 min, resuspended in LB, and allowed to sit on ice for 5 min. This was centrifuged at 1000 *g* for 10 min, resulting in a pellet (P2) containing nuclei, and a supernatant (S2) containing mitochondria. S2 was centrifuged at 1000 *g* for 10 min to pellet nuclear contamination, with the resulting supernatant kept as the mitochondrial-enriched fraction. The P2 pellet was resuspended in LB, centrifuged at 1000 *g* for 10 min, again suspended in LB, sonicated for 20 s, and kept as the nuclear-enriched fraction.

Protein content of whole cell lysates and fractions was determined using the BCA protein assay method. Subcellular fraction purity was validated by immunoblotting for actin (cytosol), MnSOD (mitochondria), and histone H2B (nucleus).

2.3. Immunoblotting

Immunoblotting was performed as previously described [22]. Membranes were probed with primary antibodies against AIF, Apaf1, ARC, ANT, Bcl-2, Bax, cytochrome c, MDM2, MyoD, p53 (Santa Cruz), histone H2B, MnSOD, Smac, XIAP (Enzo Life Sciences), myosin, myogenin (Developmental Studies Hybridoma Bank), actin (Sigma Aldrich), FLAG, HA (Cell Signaling), or PUMA (Abcam). Membranes were then incubated with the appropriate horseradish peroxidase (HRP)-conjugated secondary antibody (Santa Cruz), and bands were visualized using enhanced chemiluminescence (ECL) immunoblotting detection reagents (BioVision) and the ChemiGenius 2 Bio-Imaging System (Syngene). The approximate molecular weight for each protein was estimated using Precision Plus Protein WesternC Standards and Precision Protein Strep-Tactin HRP Conjugate (Bio-Rad Laboratories). Equal loading and quality of transfer were confirmed by staining membranes with Ponceau S (Sigma Aldrich).

2.4. Caspase activity

Enzymatic activity of caspase-2, -3, -8, and -9 was determined using the substrates Ac-VDVAD-AMC, Ac-DEVD-AMC, Ac-IETD-AMC, and Ac-LEHD-AMC (Enzo Life Sciences), respectively [22]. Cells were isolated as mentioned above using LB without addition of protease inhibitors, and incubated in duplicate in black 96-well plates with the appropriate fluorogenic substrate at room temperature. Fluorescence was measured with excitation and emission wavelengths of 360 nm and 440 nm, respectively. Caspase activity was normalized to total protein content and expressed as fluorescence intensity in arbitrary units (AU) per milligram protein.

2.5. Transfections and plasmids

C2C12 cells were transfected with various plasmids (Addgene) to modify XIAP expression. Transfections were performed with Lipofectamine 2000 (Life Technologies) optimized according to the manufacturer's instructions. A transfection efficiency of 50–60% was generally achieved. Cells were transfected upon reaching 50–60% confluence and differentiation was induced the following day. Plasmids used included: pEBB-FLAG-XIAP (encoding full-length human XIAP protein, hXIAP), pEBB-FLAG-XIAP-D148A (mutation which prevents XIAP from binding caspase-3), pEBB-HA-XIAP-H467A (mutation which prevents XIAP's E3 ubiquitin ligase activity), and pEBB-GFP (control).

C2C12 cells stably expressing GFP-tagged cytochrome c (Cytc-GFP) were generated using retroviral transduction. Briefly, Phoenix helper-free retrovirus packaging cells were transfected as outlined above with pCytochrome C-GFP [24]. Two days post-transfection, Phoenix cell media was harvested, filtered, and used to transduce C2C12 cells. Stably transduced Cytc-GFP expressing C2C12 clones were selected with puromycin (Sigma Aldrich).

2.6. Immunofluorescent and live-cell microscopy

Fluorescent microscopy was used to visualize nuclei and expression of myosin. Cells grown on gelatin-coated glass coverslips were removed from culture at appropriate time points and incubated with a myosin-specific antibody (Developmental Studies Hybridoma Bank) diluted in 10% goat serum in PBS for 1 h. Cells were then incubated with a fluorescent-conjugated secondary antibody (Santa Cruz) for 1 h, counterstained with DAPI (Life Technologies) to identify nuclei, and mounted with Prolong Gold Antifade Reagent (Life Technologies). Images were captured with an Axio Observer Z1 fluorescent microscope equipped with standard Red/Green/Blue filters, an AxioCam HRm camera, and AxioVision software (Carl Zeiss).

Cytochrome c visualization was performed in live C2C12 cells stably expressing Cytc-GFP (detailed above) using the aforementioned fluorescent microscope with optical sectioning through structured illumination (Carl Zeiss). Live imaging was performed in a temperature- and humidity-controlled microscope-mounted chamber maintained at 37 °C and 5% CO_2.

2.7. Cell fusion index

Images stained with myosin and DAPI were used to determine the degree of myoblast fusion by counting all nuclei in five random microscopic fields per experiment. Nuclei were categorized as follows: single-nucleated myosin negative (unfused), single-nucleated myosin positive (unfused with myosin), or multi-nucleated myosin positive (fused).

2.8. Flow cytometry

Cells were harvested as described above and suspended in Hank's Balanced Salt Solution (HBSS). Mitochondrial membrane potential and mitochondrial permeability transition pore formation were measured using JC-1 and calcein, respectively, as previously performed [22]. Mitochondrial membrane depolarization can be monitored by changes in the JC-1 red:green fluorescence ratio, where a decreased ratio is indicative of decreased mitochondrial membrane potential. Briefly, cells were incubated with 2 μM JC-1 in HBSS for 15 min at 37 °C, washed by centrifugation, and resuspended in HBSS. As a positive control for membrane depolarization, cells were incubated with JC-1 and the mitochondrial uncoupler CCCP (Enzo Life Sciences). Mitochondrial permeability transition pore (mPTP) formation occurs during mitochondrial-mediated apoptosis prior to mitochondrial apoptotic protein release. The fluorescent dye calcein AM accumulates in intact mitochondria, but is quenched by cobalt if the mitochondrial membrane becomes permeable to cobalt. Thus a decrease in calcein fluorescence indicates mPTP formation. Briefly, cells were incubated with 1 μM calcein AM and 1 mM $CoCl_2$ in HBSS for 15 min at 37 °C, washed by centrifugation, and resuspended in 500 μL HBSS.

For analysis of Ac-DEVD-CHO toxicity, Annexin-V/PI staining was performed [22]. After treatment, cells were suspended in buffer (10 mM HEPES/NaOH, 150 mM NaCl, 1.8 mM $CaCl_2$, pH 7.4) and incubated with 5 μL of Annexin V-FITC (Life Technologies) and 1 μL of 500 μg/mL propidium iodide (PI). There were no differences in the number of healthy or dead cells as measured using Annexin V/PI staining in cells incubated with Ac-DEVD-CHO for up to 2 days (*data not shown*). All analyses were performed on a flow cytometer (BD FACSCalibur) equipped with Cell Quest Pro software (BD Bioscience).

2.9. DNA fragmentation

Cytoplasmic histone-associated mono- and oligonucleosomes were determined using the Cell Death Detection ELISA^{PLUS} Kit (Roche) as

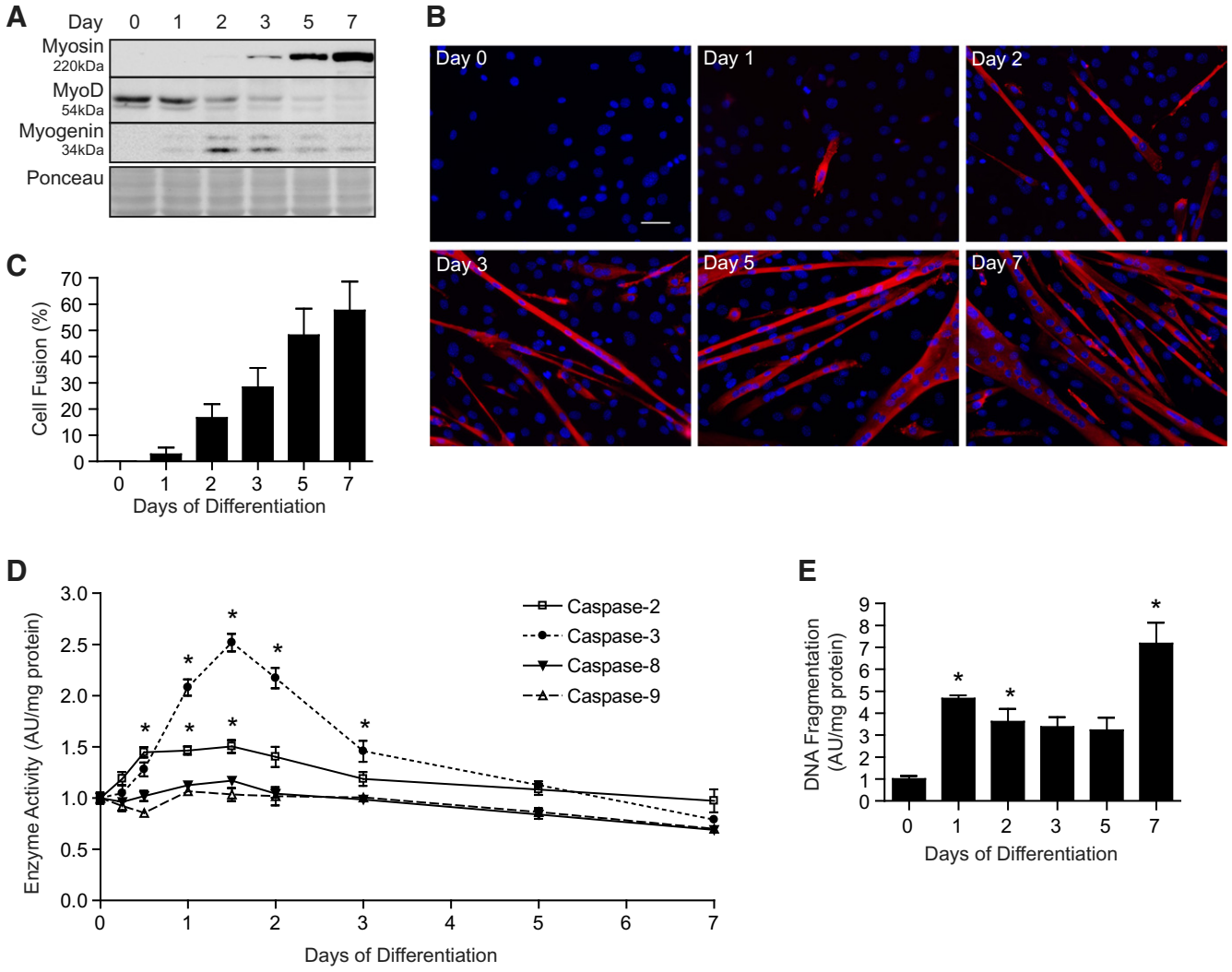

Fig. 1. C2C12 differentiation is associated with temporary activation of caspases. (A) Protein expression of skeletal muscle differentiation markers. (B and C) Representative images of myosin (red) and nuclei (blue) immunofluorescent staining demonstrating progressive increase in myotube formation and quantification of cell fusion. Scale bar = 50 μm. (D) Caspase-2 and -3 activities were temporarily elevated during differentiation. (E) DNA fragmentation in adhered cells was increased early and late during differentiation. *$p < 0.05$ compared to day 0.

previously reported [22]. Briefly, cells (1×10^4) were incubated in the supplied lysis buffer and centrifuged at 200 *g* for 10 min. Supernatant was incubated with anti-histone-biotin/anti-DNA-POD reagent in a streptavidin-coated microplate for 2 h at room temperature under gentle shaking. The solution was then removed, wells were washed several times, and 100 mL of ABTS substrate solution was added to each well. As a control for DNA fragmentation, a sample containing a DNA–histone-complex was included and produced a strong positive signal. Absorbance was measured at 405 nm and 490 nm and normalized to total protein content and expressed as AU per mg protein.

2.10. Cell counting/size analysis

Cell counts were performed with a Z2 Coulter Counter (Beckman–Coulter) to ensure accurate seeding densities and assess the number of dead cells contained in culture media. Cells between 12–19 μm were considered viable and plated at appropriate densities and dead cells were determined by counting events between 5–12 μm.

2.11. Statistical analyses

All results shown are means ± standard error of the mean (s.e.m.), where $n = 3$ for each experiment. Data were analyzed using one-way ANOVA and Tukey's post-hoc analysis with $p < 0.05$ considered statistically significant. For experiments characterizing apoptotic signaling during differentiation, comparisons were made between day 0 and each subsequent time point. For other experiments, comparisons were made between indicated treatment groups. Analyses were performed using GraphPad Prism.

3. Results

3.1. C2C12 differentiation is associated with temporary activation of caspases

Switching C2C12 cells to DM induced typical differentiation-associated changes such as progressively increased myosin, decreased MyoD, and transient myogenin protein expression (Fig. 1A). Additionally, immunofluorescent microscopy of myosin showed that myotube development peaked on day 7, where 57% of nuclei were contained in multi-nucleated cells (Fig. 1B,C). The transient activation of caspase-3 typical of differentiation was also observed (Fig. 1D). In contrast with previous reports [20,21], significant changes to caspase-8 and -9 activities did not occur (Fig. 1D). However, caspase-2 activity increased 0.5 days after inducing differentiation, and remained elevated by 45–51% ($p < 0.05$) until day 1.5 (Fig. 1D). Finally, although this temporary caspase activity has been suggested to be too low to cause damaging apoptotic features, the level of DNA fragmentation in adhered cells was elevated ($p < 0.05$) 4.6-fold and 3.6-fold, respectively, on days 1 and 2 of differentiation (Fig. 1E). The increase ($p < 0.05$) in DNA fragmentation observed on day 7 is likely a consequence of the time spent in culture.

3.2. Changes to pro- and anti-apoptotic proteins during differentiation

Differentiation was associated with the rapid appearance of p53 and the disappearance of MDM2, a ubiquitin ligase which targets p53 (Fig. 2A,B). Two genes controlled by p53 are the pro-apoptotic Bcl-2 family members Bax and PUMA [25,26]. The protein expression of Bax and PUMA was increased ($p < 0.05$) 16% and 23%, respectively, on day 1 compared to day 0 (Fig. 2A,C). However, the expression of Apaf1, a protein which contributes to caspase-9 activation, did not change

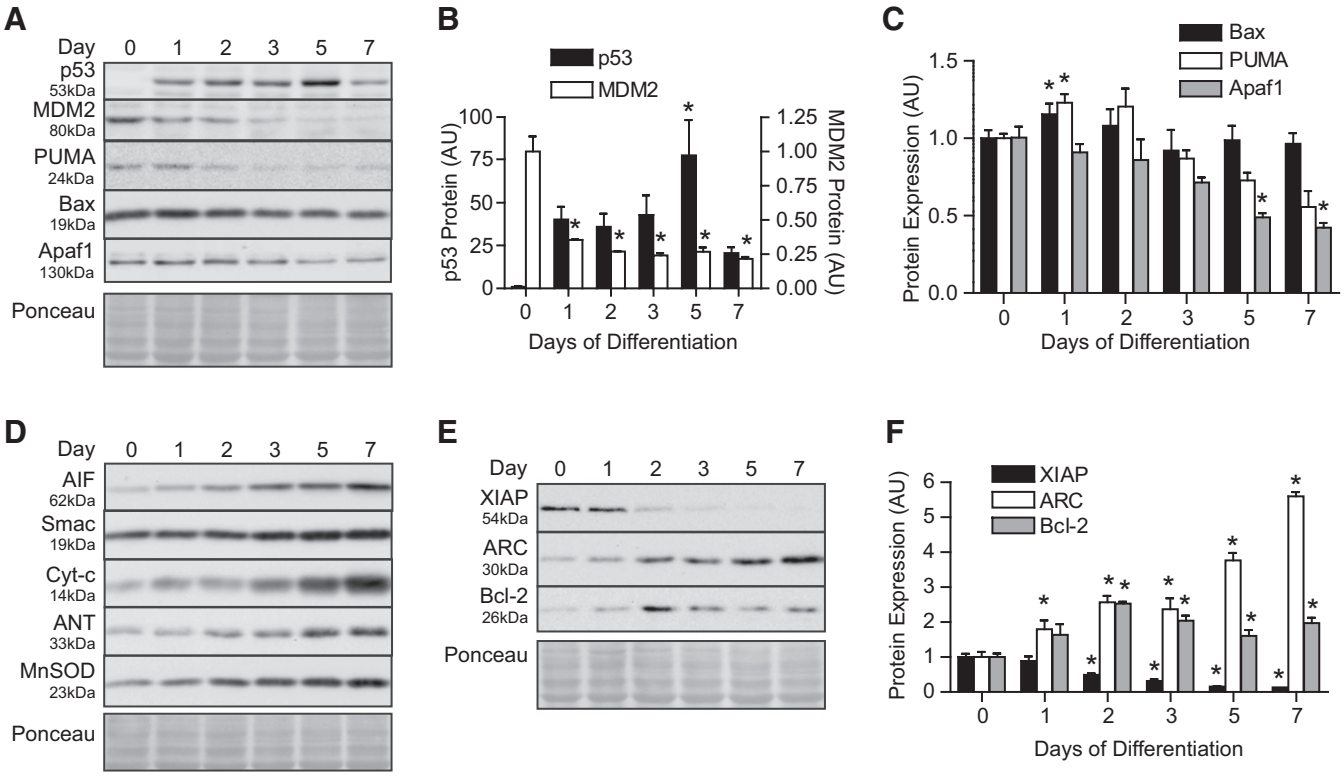

Fig. 2. Changes to pro- and anti-apoptotic proteins during differentiation. (A and B) Differentiation was associated with the appearance of p53 and the progressive decline of its ubiquitin ligase MDM2. (A and C) PUMA and Bax protein were elevated on day 1 of differentiation, while Apaf1 was decreased on days 5 and 7. (D) The expression of mitochondrial pro-apoptotic proteins increased along with markers of mitochondrial content. (E and F) Expression of anti-apoptotic proteins varied throughout differentiation. *$p < 0.05$ compared to day 0.

early during differentiation, but decreased progressively reaching significance ($p < 0.05$) on days 5 and 7 (Fig. 2A,C). In addition, the protein levels of several mitochondrial pro-apoptotic factors (AIF, Smac, cytochrome c) changed similarly to markers of mitochondrial content (ANT, MnSOD), which is known to increase during myotube development [27] (Fig. 2D). The expression of two anti-apoptotic proteins (Bcl-2 and ARC) which can act upstream of mitochondrial disruption was elevated ($p < 0.05$) as caspase activity decreased, with Bcl-2 increasing 2.5-fold by day 2 of differentiation and ARC progressively increasing 5.6-fold by day 7 (Fig. 2E,F). Importantly, XIAP, which acts downstream of the mitochondria by inhibiting caspases, decreased ($p < 0.05$) by 51% by day 2 and continued to decline throughout differentiation (Fig. 2E,F).

3.3. Markers of mitochondrial-mediated apoptosis do not increase following the induction of differentiation

As the functional relevance of several apoptosis-regulating factors depends on their cellular localization, we next examined the content of select proteins in subcellular fractions. Although whole-cell (Fig. 2A, C) and mitochondrial (Fig. 3A) Bax increased ($p < 0.05$) 1 day after inducing differentiation, mitochondrial Bax was matched by Bcl-2 during the early days of differentiation, resulting in no change to the Bax:Bcl-2 ratio (Fig. 3A,B). This result suggests that any apoptotic action of Bax was likely inhibited prior to caspase activation. In accordance with this, mitochondrial permeability transition pore (mPTP) formation did not increase early during differentiation (Fig. 3C). In fact, calcein

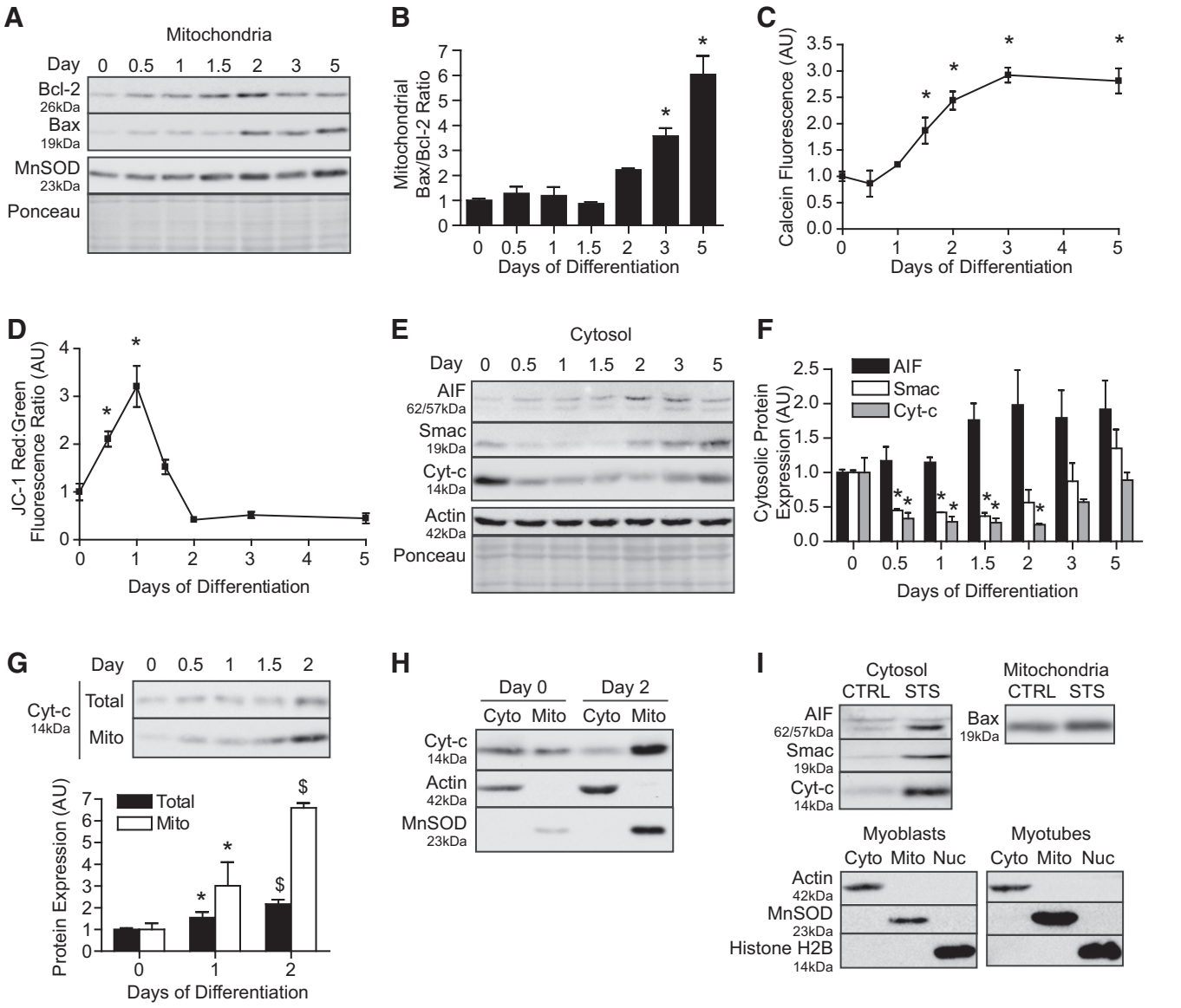

Fig. 3. Markers of mitochondrial-mediated apoptosis do not increase following the induction of differentiation. (A and B) The Bax:Bcl-2 ratio in mitochondrial-enriched fractions did not change early during differentiation. (C) Calcein fluorescence increased midway through the differentiation process, likely due to elevated mitochondrial content. (D) Mitochondrial membrane potential was transiently increased early during differentiation. (E and F) Cytosolic levels of Smac and cytochrome c, but not AIF, rapidly dropped 0.5 days after the induction of differentiation. (G) Cytochrome c expression in mitochondrial-enriched fractions (Mito) increased to a greater extent than in whole-cell lysates (Total) during the first 2 days of differentiation. (H) Equal amounts of cytosolic (Cyto) and mitochondrial (Mito) fraction extracts were immunoblotted to demonstrate the relative expression level of cytochrome c. Its redistribution during the first 2 days of differentiation is readily apparent. (I) Validation that subcellular fractions detected appropriate apoptotic signaling. C2C12 cells were treated with 2 μM staurosporine (STS) for 3 h and fractions were attained as outlined in Materials and methods. Also shown are representative immunoblots demonstrating fraction purity. $^{*}p < 0.05$ compared to day 0; $^{\$}p < 0.05$ compared to all other days.

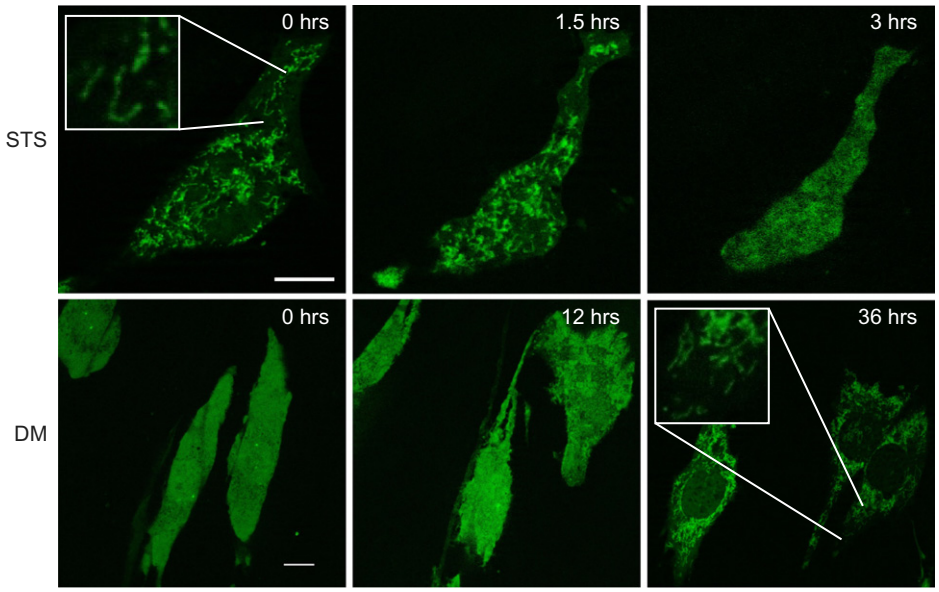

Fig. 4. Translocation of Cytc-GFP in stably transduced C2C12 cells. Top panels: Time-lapse images showing staurosporine (STS)-induced mitochondrial Cytc-GFP release. Bottom panels: Time-lapse images demonstrating mitochondrial-localization of Cytc-GFP during the first 36 h of differentiation (DM). Scale bars = 10 μm.

fluorescence increased ($p < 0.05$) midway through the differentiation process, likely due to elevated mitochondrial content (Fig. 3C). Additionally, mitochondrial membrane potential transiently increased ($p < 0.05$) up to 3.2-fold by day 1 of differentiation (Fig. 3D).

Ultimately, mitochondrial disruption stimulates apoptosis by releasing several cell death promoting proteins. Cytosolic levels of Smac and cytochrome c declined ($p < 0.05$) 55% and 60%, respectively, on day 0.5 and remained lowered during the spike in caspase activity (Fig. 3E, F). Similar changes to AIF localization were not observed (Fig. 3E,F). Interestingly, although total cytochrome c protein levels increased 2.1-fold in the first 2 days of differentiation similar to the mitochondrial markers MnSOD and ANT (Fig. 2D), mitochondrial-specific cytochrome c was elevated 6.6-fold (Fig. 3G). In fact, immunoblotting with equal amounts of cellular extract demonstrated that cytochrome c became less cytosolic and more mitochondrial-localized early during differentiation (Fig. 3H). To ensure that subcellular fractions detected proper apoptotic signaling, C2C12 cells were treated with 2 μM staurosporine (STS) for 3 h. As shown, STS resulted in elevated cytosolic AIF (the 57 kDa isoform), Smac, and cytochrome c, as well as increased mitochondrial Bax compared to untreated cells (CTRL) (Fig. 3I).

3.4. Translocation of Cytc-GFP in stably transduced C2C12 cells

The decrease in cytosolic cytochrome c was further illustrated in C2C12 cells stably expressing a GFP-cytochrome c fusion protein (Cytc-GFP). Notably, we found that in stably selected clones, myoblasts with mitochondrial-localized GFP were rare (see Fig. 4, bottom left panel). However, time-lapse imaging of live cells with mitochondrial-GFP revealed that treatment with staurosporine (STS, 2 μM, 3 h) appropriately induced Cytc-GFP release (Fig. 4, top panels). Most importantly, during the first 1.5 days of differentiation, Cytc-GFP became mitochondrial-localized in myoblasts with initially non-mitochondrial Cytc-GFP expression (Fig. 4, bottom panels).

3.5. Mitochondrial hyperpolarization stimulates cytochrome c translocation to the mitochondria

The observation that differentiation was associated with transiently increased mitochondrial membrane potential and reduced cytosolic levels of cytochrome c was not expected, thus we examined whether these events were related. Incubation of cells with CCCP dramatically

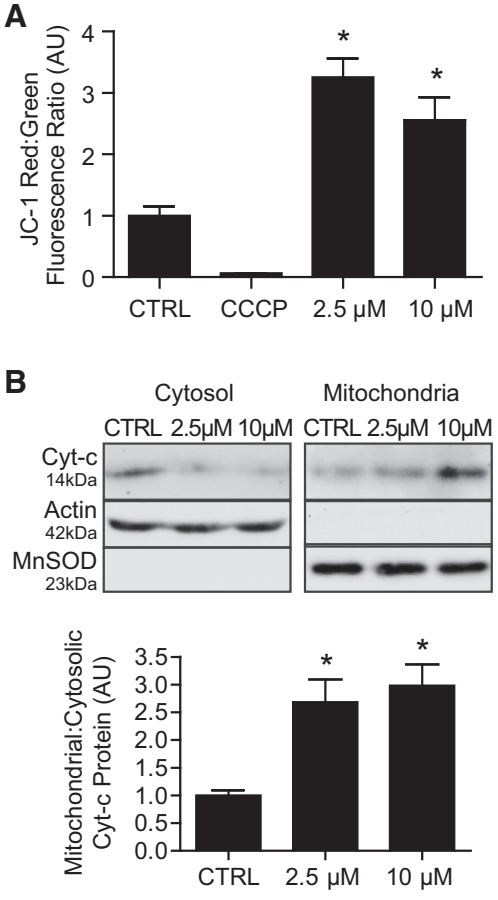

Fig. 5. Mitochondrial hyperpolarization stimulates cytochrome c translocation to the mitochondria. Subconfluent C2C12 cells were treated for 6 h with the indicated concentrations of oligomycin. (A) Oligomycin increased mitochondrial membrane potential as demonstrated by JC-1 red:green fluorescence ratio. CCCP represents control cells incubated with both JC-1 and CCCP. (B) Reduced cytosolic and increased mitochondrial cytochrome-c protein levels with oligomycin treatment. *$p < 0.05$ compared to control.

induced mitochondrial membrane depolarization (as seen by a decrease in the JC-1 red:green ratio). C2C12 cells treated for 6 h with 2.5 μM or 10 μM oligomycin, an ATP synthase inhibitor, displayed increased ($p < 0.05$) red:green fluorescence ratio of JC-1 by 3.3-fold and 2.6-fold, respectively, indicating mitochondrial hyperpolarization (Fig. 5A). Furthermore, oligomycin treatment resulted in decreased cytosolic and increased mitochondrial cytochrome c protein levels (Fig. 5B). As a result, the ratio of mitochondrial to cytosolic cytochrome c protein increased ($p < 0.05$) 2.7-fold and 3.0-fold in response to 2.5 μM and 10 μM oligomycin, respectively (Fig. 5B).

3.6. XIAP's E3 ubiquitin ligase activity regulates its degradation and caspase inhibitory effects during C2C12 differentiation

Given the lack of upstream mitochondrial apoptotic signaling, we examined XIAP's role in regulating caspase-3 activity and myoblast differentiation as its protein expression declined dramatically during myogenesis. C2C12 cells were transfected with specific plasmids to introduce human XIAP (hXIAP), and two XIAP mutants (D148A: impaired caspase-3 binding; H467A: deficient E3 ligase activity). Control cells were transfected with a similar vector encoding GFP. We generally achieved levels of exogenous XIAP that resulted in a 50–100% increase in total XIAP expression 24 h post transfection (Fig. 6A). Although both hXIAP and D148A were degraded on a similar timeline to endogenous XIAP (Fig. 6B,C), H467A expression was maintained during differentiation (Fig. 6B,C), suggesting that self-ubiquitination is responsible for XIAP disappearance during differentiation. While cells transfected with D148A displayed similar caspase-3 activity as GFP control cells, hXIAP induced a 57% reduction ($p < 0.05$) in total caspase-3 activity compared to controls during differentiation (Fig. 6D,E). Additionally, although we hypothesized the degradation-resistant H467A would result in an even greater inhibition of caspase-3, it reduced ($p < 0.05$) activity by 33% compared to control cells (Fig. 6D,E). In fact, this was significantly different ($p < 0.05$) than the inhibition achieved by hXIAP (Fig. 6D,E).

3.7. Reduction of caspase-3 activity with exogenous XIAP does not alter myoblast differentiation

Immunofluorescent visualization of myosin and quantification of cell fusion events after 5 days of differentiation indicated that, despite partially inhibiting caspase-3 activity, myotube formation was not prevented by XIAP transfections (Fig. 7A,B). In agreement with this, immunoblotting analyses demonstrated that the expression of muscle differentiation markers was not different between groups (Fig. 7C,D).

3.8. Complete inhibition of caspase-3 is necessary to affect myoblast differentiation

We subsequently tested whether the degree of enzyme inhibition determines the impact on myogenesis. C2C12 cells differentiated with increasing amounts of Ac-DEVD-CHO displayed progressively less ($p < 0.05$) caspase-3 activity during myogenesis (Fig. 8A). Although 5 μM and 10 μM of inhibitor did not affect myotube formation, 30 μM Ac-DEVD-CHO reduced ($p < 0.05$) cell fusion on day 5 compared to all other groups (Fig. 8B,C). Similarly, myosin protein expression was decreased ($p < 0.05$) on days 3 and 5, while myogenin was decreased ($p < 0.05$) on days 2 and 3 in cells receiving 30 μM of the inhibitor (Fig. 8D,E).

4. Discussion

In this study we investigated the biologically-relevant cause for caspase-3 activation in differentiating C2C12 myoblasts. While apoptotic signaling in differentiating skeletal muscle has been examined

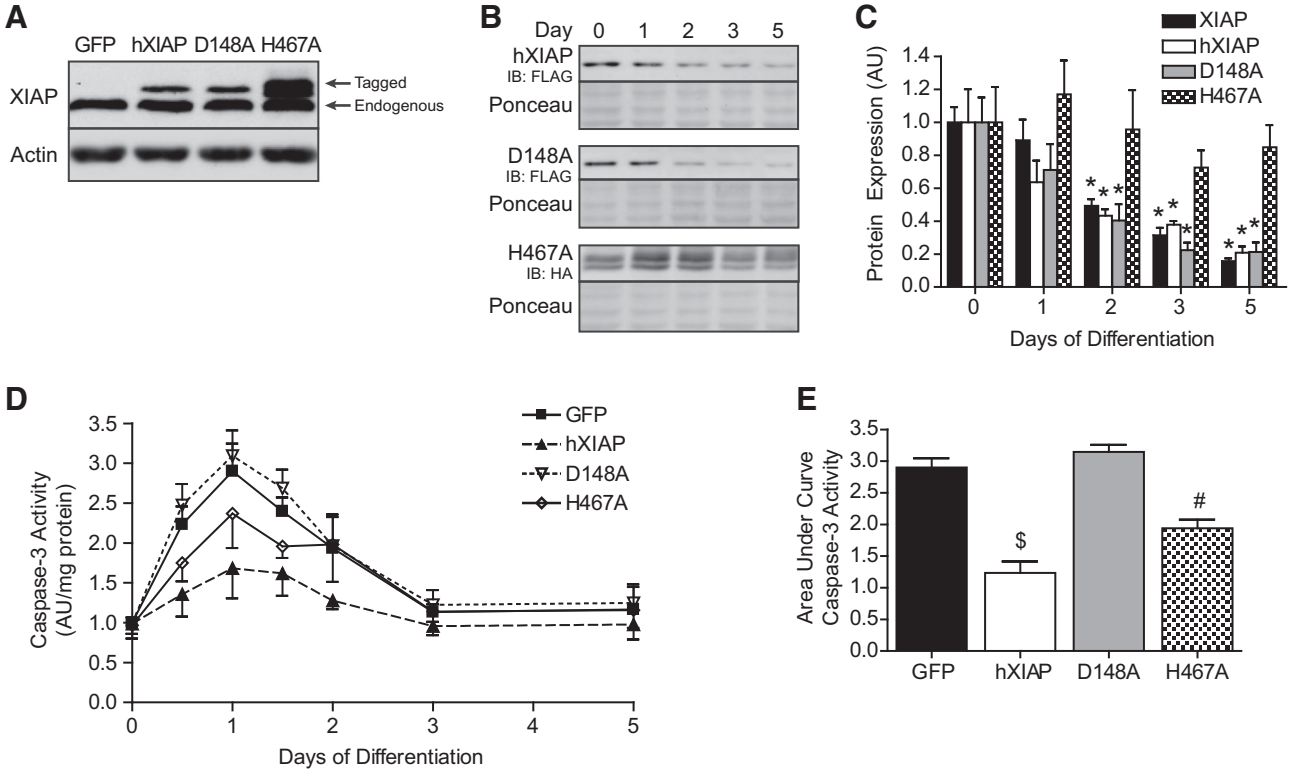

Fig. 6. XIAP's E3 ubiquitin ligase activity regulates its degradation and caspase inhibitory effects during C2C12 differentiation. See Materials and methods for transfection/plasmid details. (A) Transfections resulted in levels of exogenous XIAP that produced a 50–100% increase in total XIAP expression 24 h post transfection. (B and C) Immunoblotting for FLAG showed that hXIAP and D148A expression decreased on a timeline similar to that observed for endogenous XIAP (for comparison purposes XIAP data from Fig. 2F is shown in panel C). However, H467A levels were maintained during differentiation, as demonstrated by HA immunoblot. (D and E) Caspase-3 activity was unaffected by D148A, while H467A did not inhibit caspase-3 to the same extent as hXIAP. $^{*}p < 0.05$ compared to respective day 0; $^{\#}p < 0.05$ compared to GFP, hXIAP and D148A; $^{\$}p < 0.05$ compared GFP, D148A, and H467A.

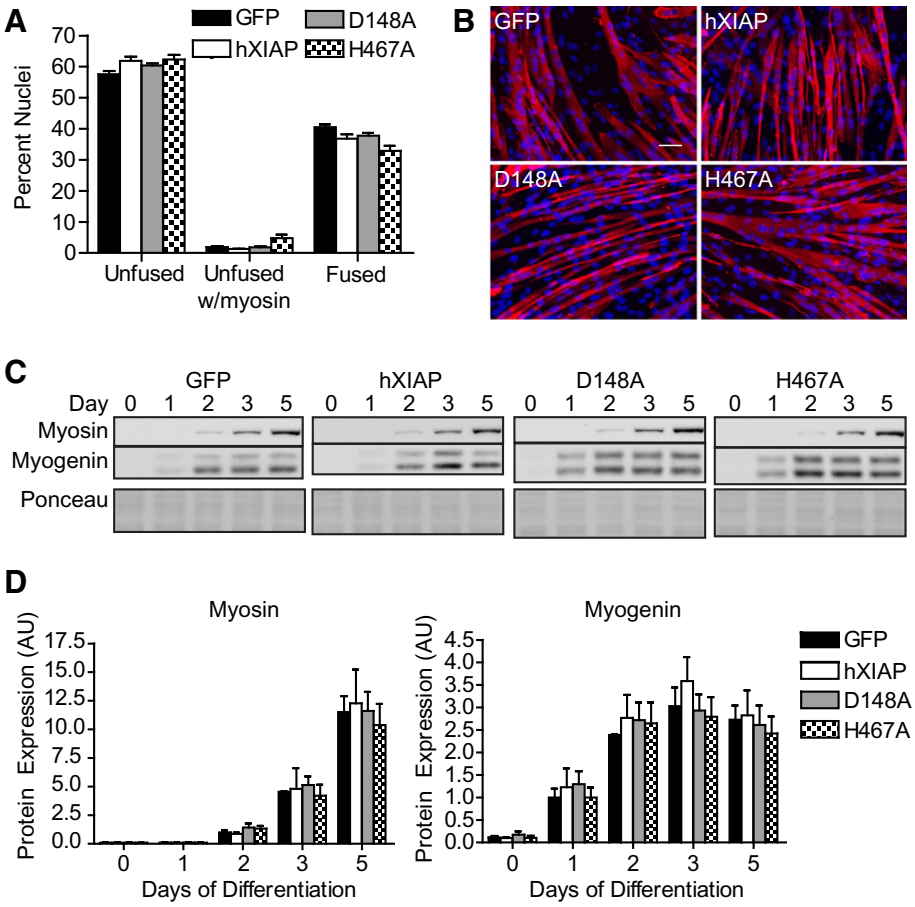

Fig. 7. Reduction of caspase-3 activity with exogenous XIAP did not alter myoblast differentiation. (A and B) Immunofluorescent identification of myosin (red) and nuclei (blue) demonstrated no effect of hXIAP or either mutant on cell fusion events on day 5 of differentiation. Scale bar = 50 μm. (C and D) Similarly, the expression of skeletal muscle differentiation markers was unaffected by XIAP overexpression.

previously, specific hallmarks such as mitochondrial permeabilization and release of pro-apoptotic factors have not been shown. Furthermore, studies have implicated specific apoptotic mechanisms without showing their respective activation in unmodified cells. Although it was hypothesized that one or more of these apoptosis-regulating mechanisms would be observed, myogenesis was associated with a reduction in several apoptosis-promoting indices.

In agreement with our initial hypothesis, caspases were transiently activated, p53-controlled pro-apoptotic proteins temporarily increased, and the decline in caspase activity coincided with increased expression of two multi-functional anti-apoptotic proteins, Bcl-2 and ARC. However, subsequent analyses did not detect elevated levels of apoptosis-promoting events, specifically those related to mitochondrial signaling.

Previously, several apoptotic mechanisms have been reported during muscle differentiation. In particular, shRNA against caspase-9 as well as Bcl-xL overexpression prevented transient caspase-3 activation and delayed cell fusion during C2C12 differentiation [20]. However, the appearance of myosin-positive myoblasts and the total protein expression of myosin and myogenin were not altered in these experiments. Using 23A2 cells, another myogenic mouse line, others have observed cytochrome c release 2 h after inducing differentiation [28]. Although, preventing cytochrome c release with shRNA-mediated PUMA knockdown as well as complete caspase-9 inhibition with a chemical enzyme inhibitor did not impair differentiation [28]. This group also showed that inhibition of caspase-8 and cells dominant negative for FADD displayed decreased myosin and MyoD protein expression, suggesting the involvement of death-receptor signaling during myoblast differentiation [21]. Despite using similar culturing techniques as Murray et al. [20], we found that Bax expression and mitochondrial translocation were matched by Bcl-2, flow cytometric analyses of calcein and JC-1 did not detect an increase in mPTP formation or a drop in mitochondrial membrane potential, cytosolic levels of cytochrome c and Smac protein dramatically decreased, and neither Apaf1 expression or caspase-9 activity increased during differentiation. These findings suggest that mitochondrial apoptotic signaling is not active in differentiating C2C12 cells. Additionally, we did not detect elevated levels of caspase-8 activity at any time point of differentiation. Indeed, these studies highlight the need to identify the mechanisms of caspase activation in unmodified differentiating muscle. In fact, while skeletal muscle development is impaired in caspase-3 knockout mice [15], caspase-9 null mice possess mature skeletal muscle [29], and mice without caspase-8 do not present with obvious skeletal muscle defects [30]. Ultimately, given the redundant cleavage-site specificities of caspases, compensatory activities may be relevant during genetic and pharmacological manipulations, perhaps leading to “delayed” instead of “prevented” muscle development phenotypes. Currently, these observations emphasize the need for subsequent analyses.

Examination of mitochondrial apoptotic signaling introduced several intriguing questions. Primarily, the dramatic reduction in cytosolic cytochrome c and Smac upon the induction of differentiation was unexpected. Previously, work has shown that these two pro-apoptotic proteins were undetectable in cytosolic fractions of subconfluent and differentiating C2C12 cells [20]. However, we detected both proteins in cytosols of untreated C2C12 cells and found that staurosporine appropriately induced mitochondrial release of both. Additionally, by stably expressing GFP-tagged cytochrome c in C2C12 cells, live-cell imaging revealed increased mitochondrial localization of Cytc-GFP during differentiation. Typically, mitochondrial depolarization is associated with the

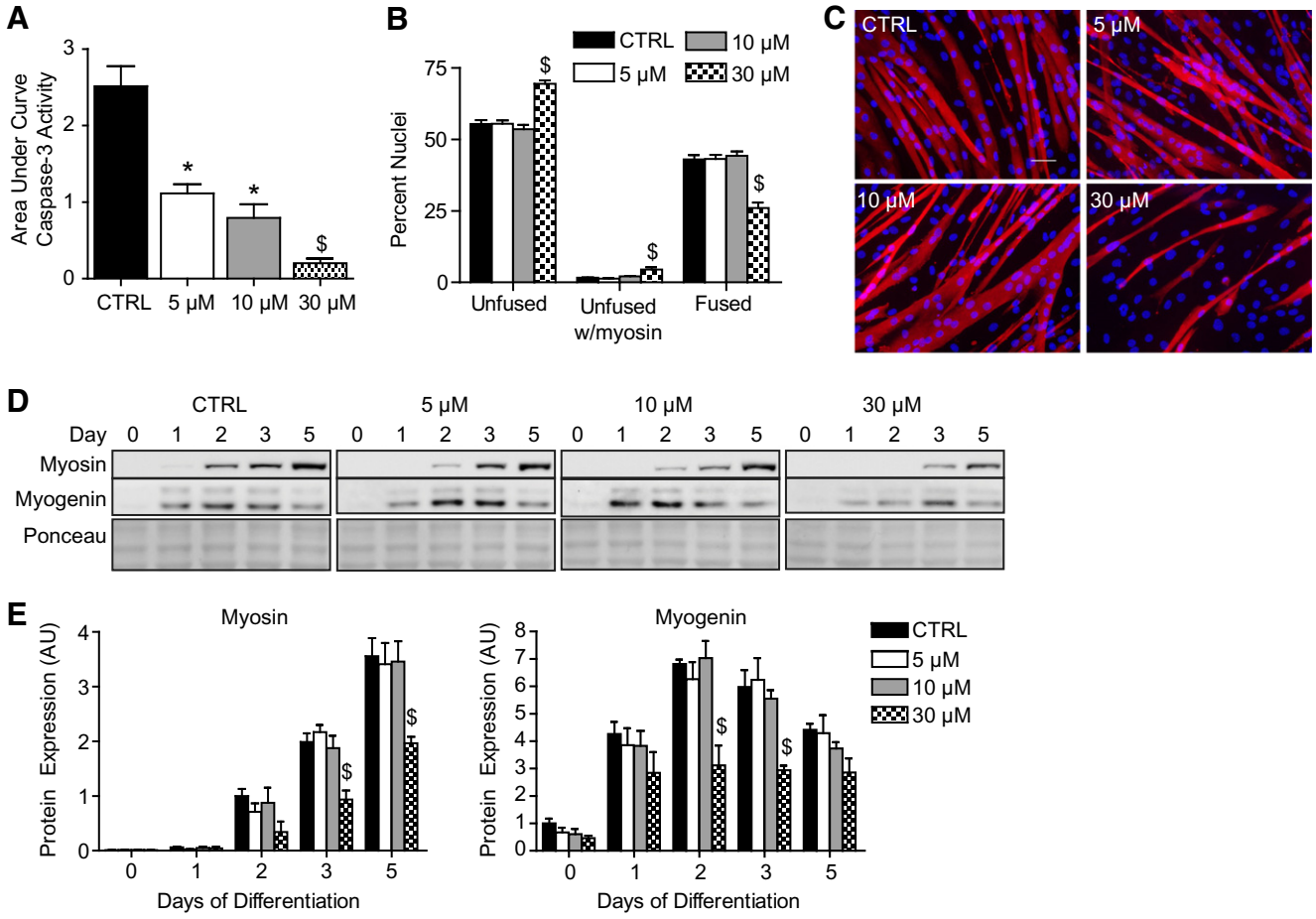

Fig. 8. Complete inhibition of caspase-3 is necessary to affect myoblast differentiation. C2C12 cells were differentiated with DM (control), or DM supplemented with the indicated concentrations of the caspase-3 inhibitor Ac-DEVD-CHO. (A) These concentrations resulted in progressively less caspase-3 activity during differentiation. (B and C) Cell fusion on day 5 was only blunted by 30 μM Ac-DEVD-CHO. Scale bar = 50 μm. (D and E) Similarly, myosin and myogenin protein expression was reduced in cells which received 30 μM Ac-DEVD-CHO. $^{*}p < 0.05$ compared to control; $^{\$}p < 0.05$ compared to all.

release of cytochrome c. Interestingly, we observed transient mitochondrial hyperpolarization immediately after inducing differentiation, so we tested whether the opposite could be true. In fact, causing mitochondrial hyperpolarization by treating subconfluent C2C12 cells with oligomycin for 6 h reduced cytosolic and increased mitochondrial cytochrome c levels. Previously, oligomycin has been shown to prevent cytochrome c release by a variety of apoptotic stressors [31,32]. Likely, oligomycin introduces an energy stress, and cells move cytochrome c to the mitochondria to promote electron transport and ATP production. Interestingly, oligomycin has also been shown to modestly raise cardiolipin content in yeast [33]. Given cytochrome c's positive charge [34], mitochondrial hyperpolarization could attract nearby cytosolic cytochrome c proteins directly, functioning to mitigate short-term energy need. Perhaps, myoblasts undergo a similar stress upon the induction of differentiation, resulting in cytochrome c redistribution.

The absence of mitochondrial apoptotic signaling and activation of typical initiator caspases in our experiments was surprising and suggests an alternative mechanism of caspase-3 activation during C2C12 differentiation. Our results show that early during differentiation there is an elevation in caspase-2, which has been shown to activate caspase-3 directly through pro-domain interactions [35]. Further, another initiator caspase, caspase-12, has been shown to be activated during myogenesis [36]. Thus, these upstream caspases may contribute to caspase-3 processing during muscle differentiation. Another possibility is regulation of caspase-3 without the involvement of upstream apoptotic signaling and activation of initiator caspases. Indeed, several protein families interact with caspases directly, and caspase function is additionally regulated by post-translational modifications such as phosphorylation and ubiquitination [37]. Potentially, any of these factors may modulate the cellular pool of caspase-3 during myogenesis and lead to increased enzyme activity. Our findings show that the protein expression of the anti-apoptotic factors Bcl-2, ARC, and XIAP changes in specific patterns during C2C12 differentiation. Most intriguing of these is XIAP, a cytosolic anti-apoptotic protein which inhibits the processing and/or enzymatically active forms of caspases-3, -7, and -9 [38]. Since XIAP expression decreased during C2C12 differentiation, we tested whether this contributes to caspase-3 activation by overexpressing normal and mutated XIAP proteins. Interestingly, XIAP regulates its own degradation through self-ubiquitination, which is made possible due to a C-terminal RING domain [39]. Furthermore, mutated or partial XIAP proteins containing dysfunctional RINGs impart protein stability during situations of induced degradation [39,40]. Therefore, we examined the effects on caspase-3 activation and myoblast differentiation caused by full-length human XIAP (hXIAP) and XIAP-H467A, a point-mutant which maintains its caspase binding abilities but has deficient E3 ligase activity [39,41].

Compared to E3-competent mutants, which followed a pattern of decreased expression similar to endogenous XIAP, protein levels were maintained in H467A transfected cells during differentiation, suggesting that self-ubiquitination contributes to declining XIAP content. In fact, elevated proteasomal activity is required for myogenesis [42,43], and numerous proteins, such as Pax3, MyoD, and Id1, are specifically targeted or protected from degradation during myogenesis [44,45]. Although declining XIAP levels could be explained by depressed protein synthesis,

our analysis of FLAG/HA tagged proteins confirms that post-translational alterations contribute to reducing XIAP expression during muscle differentiation. Therefore, it is likely that the E3-ligase activity of XIAP or its susceptibility to ubiquitination is modulated during differentiation by an unknown mechanism. Interestingly, we observed decreased cytosolic Smac levels immediately after inducing differentiation. Given that Smac is a primary regulator of XIAP function and ligase activity [46], this effect would tend to promote XIAP's ligase activity and anti-apoptotic abilities. Furthermore, XIAP is regulated by many growth and stress signaling pathways including AKT, JNK, and ERK/MAPK [47–49], several of which are involved with or altered during C2C12 differentiation [50].

Transfection of hXIAP resulted in less caspase-3 activity during differentiation compared to H467A. It was hypothesized that H467A would cause more caspase inhibition, as its protein levels were maintained during differentiation, and XIAP stability has been correlated with its anti-apoptotic effectiveness [39]. However, in addition to targeting itself for ubiquitination, XIAP functions as an E3-ligase for caspase-3 [51], caspase-9 [52], and Smac [53], among others. As a result, XIAP's ubiquitin ligase activity has been shown to be important for its anti-apoptotic effects [40,51]. Therefore, XIAP-dependent caspase-3 ubiquitination may be relevant for its caspase-inhibiting functions during periods of prolonged stress, such as that which occurs during myogenesis.

Previous studies have demonstrated that various modes of caspase inhibition prevent or delay muscle differentiation [15,19–21,54]. As such, administering a high concentration of Ac-DEVD-CHO completely prevented caspase-3 activation and subsequently impaired myogenesis. However, while caspase-3 activity was decreased in C2C12 cells with hXIAP and H467A overexpression, differentiation was unaffected. This is likely a result of insufficient enzyme inhibition, as in experiments where modest caspase-3 reduction was achieved with Ac-DEVD-CHO treatment, myotube development occurred normally.

The D148A variant was selected to isolate the effect of caspase-3 inhibition. This point-mutation lies in XIAP's Linker-BIR2 region, which is required for caspase-3 interaction [51,55]. Importantly, this mutated XIAP features an intact BIR3 domain, and therefore maintains caspase-9 binding ability [56]. When transfected into C2C12 cells prior to differentiation, D148A did not reduce total caspase-3 activity compared to control cells transfected with GFP. This finding provides additional evidence supporting our conclusion that caspase-3 is not activated by mitochondrial/caspase-9 apoptotic signaling during C2C12 differentiation.

5. Conclusion

This study serves as a comprehensive analysis of apoptotic effector signaling during C2C12 differentiation. We found that mitochondrial-mediated apoptotic signaling mechanisms did not precede the transient caspase-3 activity associated with myogenesis. Additionally, XIAP overexpression did not impair myoblast differentiation, suggesting that its degradation is likely not responsible for caspase activation in this context. These findings emphasize the complex relationship between cell death and differentiation, and provide the basis for future research.

Author contributions

D.B. performed the experimental and data analyses. D.B. and J.Q. designed the experiments and wrote the manuscript.

Acknowledgements

The authors thank Dr. D.R. Green, St Jude's Children's Research Hospital, Memphis, Tennessee for providing pCytochrome C-GFP. This research was supported by funds provided by the Natural Sciences and Engineering Research Council of Canada (341256) to Joe Quadrilatero.

References

[1] P. Saikumar, Z. Dong, V. Mikhailov, M. Denton, J.M. Weinberg, M.A. Venkatachalam, Apoptosis: definition, mechanisms, and relevance to disease, Am. J. Med. 107 (1999) 489–506.
[2] C. Du, M. Fang, Y. Li, L. Li, X. Wang, Smac, a mitochondrial protein that promotes cytochrome c-dependent caspase activation by eliminating IAP inhibition, Cell 102 (2000) 33–42.
[3] P. Li, D. Nijhawan, I. Budihardjo, S.M. Srinivasula, M. Ahmad, E.S. Alnemri, X. Wang, Cytochrome c and dATP-dependent formation of Apaf-1/caspase-9 complex initiates an apoptotic protease cascade, Cell 91 (1997) 479–489.
[4] Z.N. Oltvai, C.L. Milliman, S.J. Korsmeyer, Bcl-2 heterodimerizes in vivo with a conserved homolog, Bax, that accelerates programmed cell death, Cell 74 (1993) 609–619.
[5] C. Scaffidi, S. Fulda, A. Srinivasan, C. Friesen, F. Li, K.J. Tomaselli, K.M. Debatin, P.H. Krammer, M.E. Peter, Two CD95 (APO-1/Fas) signaling pathways, EMBO J. 17 (1998) 1675–1687.
[6] C. Garrido, G. Kroemer, Life's smile, death's grin: vital functions of apoptosis-executing proteins, Curr. Opin. Cell Biol. 16 (2004) 639–646.
[7] L.A. Sabourin, M.A. Rudnicki, The molecular regulation of myogenesis, Clin. Genet. 57 (2000) 16–25.
[8] A.B. Lassar, S.X. Skapek, B. Novitch, Regulatory mechanisms that coordinate skeletal muscle differentiation and cell cycle withdrawal, Curr. Opin. Cell Biol. 6 (1994) 788–794.
[9] T.J. Harford, A. Shaltouki, C.M. Weyman, Increased expression of the pro-apoptotic Bcl2 family member PUMA and apoptosis by the muscle regulatory transcription factor MyoD in response to a variety of stimuli, Apoptosis 15 (2010) 71–82.
[10] H. Hirai, M. Verma, S. Watanabe, C. Tastad, Y. Asakura, A. Asakura, MyoD regulates apoptosis of myoblasts through microRNA-mediated down-regulation of Pax3, J. Cell Biol. 191 (2010) 347–365.
[11] G. Qu, H. Yan, A.R. Strauch, Actin isoform utilization during differentiation and remodeling of BC3H1 myogenic cells, J. Cell. Biochem. 67 (1997) 514–527.
[12] T. Yagami-Hiromasa, T. Sato, T. Kurisaki, K. Kamijo, Y. Nabeshima, A. Fujisawa-Sehara, A metalloprotease-disintegrin participating in myoblast fusion, Nature 377 (1995) 652–656.
[13] S.M. van den Eijnde, M.J. van den Hoff, C.P. Reutelingsperger, W.L. van Heerde, M.E. Henfling, C. Vermeij-Keers, B. Schutte, M. Borgers, F.C. Ramaekers, Transient expression of phosphatidylserine at cell–cell contact areas is required for myotube formation, J. Cell Sci. 114 (2001) 3631–3642.
[14] P. Fernando, L.A. Megeney, Is caspase-dependent apoptosis only cell differentiation taken to the extreme? FASEB J. 21 (2007) 8–17.
[15] P. Fernando, J.F. Kelly, K. Balazsi, R.S. Slack, L.A. Megeney, Caspase 3 activity is required for skeletal muscle differentiation, Proc. Natl. Acad. Sci. U. S. A. 99 (2002) 11025–11030.
[16] S. Demontis, C. Rigo, S. Piccinin, M. Mizzau, M. Sonego, M. Fabris, C. Brancolini, R. Maestro, Twist is substrate for caspase cleavage and proteasome-mediated degradation, Cell Death Differ. 13 (2006) 335–345.
[17] D.B. Spicer, J. Rhee, W.L. Cheung, A.B. Lassar, Inhibition of myogenic bHLH and MEF2 transcription factors by the bHLH protein Twist, Science 272 (1996) 1476–1480.
[18] L. de la Vega, J. Hornung, E. Kremmer, M. Milanovic, M.L. Schmitz, Homeodomain-interacting protein kinase 2-dependent repression of myogenic differentiation is relieved by its caspase-mediated cleavage, Nucleic Acids Res. 41 (2013) 5731–5745.
[19] B.D. Larsen, S. Rampalli, L.E. Burns, S. Brunette, F.J. Dilworth, L.A. Megeney, Caspase 3/caspase-activated DNase promote cell differentiation by inducing DNA strand breaks, Proc. Natl. Acad. Sci. U. S. A. 107 (2010) 4230–4235.
[20] T.V. Murray, J.M. McMahon, B.A. Howley, A. Stanley, T. Ritter, A. Mohr, R. Zwacka, H.O. Fearnhead, A non-apoptotic role for caspase-9 in muscle differentiation, J. Cell Sci. 121 (2008) 3786–3793.
[21] M. Freer-Prokop, J. O'Flaherty, J.A. Ross, C.M. Weyman, Non-canonical role for the TRAIL receptor DR5/FADD/caspase pathway in the regulation of MyoD expression and skeletal myoblast differentiation, Differentiation 78 (2009) 205–212.
[22] A.D. Dam, A.S. Mitchell, J. Quadrilatero, Induction of mitochondrial biogenesis protects against caspase-dependent and caspase-independent apoptosis in L6 myoblasts, Biochim. Biophys. Acta 1833 (2013) 3426–3435.
[23] N.J. Waterhouse, R. Steel, R. Kluck, J.A. Trapani, Assaying cytochrome C translocation during apoptosis, Methods Mol. Biol. 284 (2004) 307–313.
[24] J.C. Goldstein, N.J. Waterhouse, P. Juin, G.I. Evan, D.R. Green, The coordinate release of cytochrome c during apoptosis is rapid, complete and kinetically invariant, Nat. Cell Biol. 2 (2000) 156–162.
[25] T. Miyashita, J.C. Reed, Tumor suppressor p53 is a direct transcriptional activator of the human bax gene, Cell 80 (1995) 293–299.
[26] K. Nakano, K.H. Vousden, PUMA, a novel proapoptotic gene, is induced by p53, Mol. Cell 7 (2001) 683–694.
[27] C.D. Moyes, O.A. Mathieu-Costello, N. Tsuchiya, C. Filburn, R.G. Hansford, Mitochondrial biogenesis during cellular differentiation, Am. J. Physiol. 272 (1997) C1345–C1351.
[28] A. Shaltouki, M. Freer, Y. Mei, C.M. Weyman, Increased expression of the pro-apoptotic Bcl2 family member PUMA is required for mitochondrial release of cytochrome C and the apoptosis associated with skeletal myoblast differentiation, Apoptosis 12 (2007) 2143–2154.
[29] S. Krajewski, M. Krajewska, L.M. Ellerby, K. Welsh, Z. Xie, Q.L. Deveraux, G.S. Salvesen, D.E. Bredesen, R.E. Rosenthal, G. Fiskum, J.C. Reed, Release of caspase-9 from mitochondria during neuronal apoptosis and cerebral ischemia, Proc. Natl. Acad. Sci. U. S. A. 96 (1999) 5752–5757.
[30] E.E. Varfolomeev, M. Schuchmann, V. Luria, N. Chiannilkulchai, J.S. Beckmann, I.L. Mett, D. Rebrikov, V.M. Brodianski, O.C. Kemper, O. Kollet, T. Lapidot, D. Soffer, T.

Sobe, K.B. Avraham, T. Goncharov, H. Holtmann, P. Lonai, D. Wallach, Targeted disruption of the mouse caspase 8 gene ablates cell death induction by the TNF receptors, Fas/Apo1, and DR3 and is lethal prenatally, Immunity 9 (1998) 267–276.
[31] L.A. Shchepina, O.Y. Pletjushkina, A.V. Avetisyan, L.E. Bakeeva, E.K. Fetisova, D.S. Izyumov, V.B. Saprunova, M.Y. Vyssokikh, B.V. Chernyak, V.P. Skulachev, Oligomycin, inhibitor of the F0 part of H^+-ATP-synthase, suppresses the TNF-induced apoptosis, Oncogene 21 (2002) 8149–8157.
[32] S. Matsuyama, J. Llopis, Q.L. Deveraux, R.Y. Tsien, J.C. Reed, Changes in intramitochondrial and cytosolic pH: early events that modulate caspase activation during apoptosis, Nat. Cell Biol. 2 (2000) 318–325.
[33] V.M. Gohil, P. Hayes, S. Matsuyama, H. Schagger, M. Schlame, M.L. Greenberg, Cardiolipin biosynthesis and mitochondrial respiratory chain function are interdependent, J. Biol. Chem. 279 (2004) 42612–42618.
[34] Y.P. Ow, D.R. Green, Z. Hao, T.W. Mak, Cytochrome c: functions beyond respiration, Nat. Rev. Mol. Cell Biol. 9 (2008) 532–542.
[35] P.A. Colussi, N.L. Harvey, L.M. Shearwin-Whyatt, S. Kumar, Conversion of procaspase-3 to an autoactivating caspase by fusion to the caspase-2 prodomain, J. Biol. Chem. 273 (1998) 26566–26570.
[36] K. Nakanishi, T. Sudo, N. Morishima, Endoplasmic reticulum stress signaling transmitted by ATF6 mediates apoptosis during muscle development, J. Cell Biol. 169 (2005) 555–560.
[37] A.B. Parrish, C.D. Freel, S. Kornbluth, Cellular mechanisms controlling caspase activation and function, Cold Spring Harb. Perspect. Biol. 5 (2013), http://dx.doi.org/10.1101/cshperspect.a008672.
[38] Q.L. Deveraux, N. Roy, H.R. Stennicke, T. Van Arsdale, Q. Zhou, S.M. Srinivasula, E.S. Alnemri, G.S. Salvesen, J.C. Reed, IAPs block apoptotic events induced by caspase-8 and cytochrome c by direct inhibition of distinct caspases, EMBO J. 17 (1998) 2215–2223.
[39] Y. Yang, S. Fang, J.P. Jensen, A.M. Weissman, J.D. Ashwell, Ubiquitin protein ligase activity of IAPs and their degradation in proteasomes in response to apoptotic stimuli, Science 288 (2000) 874–877.
[40] A.J. Schile, M. Garcia-Fernandez, H. Steller, Regulation of apoptosis by XIAP ubiquitin-ligase activity, Genes Dev. 22 (2008) 2256–2266.
[41] J. Lewis, E. Burstein, S.B. Reffey, S.B. Bratton, A.B. Roberts, C.S. Duckett, Uncoupling of the signaling and caspase-inhibitory properties of X-linked inhibitor of apoptosis, J. Biol. Chem. 279 (2004) 9023–9029.
[42] Z. Cui, S.M. Hwang, A.V. Gomes, Identification of the immunoproteasome as a novel regulator of skeletal muscle differentiation, Mol. Cell. Biol. 34 (2014) 96–109.
[43] F. Gardrat, V. Montel, J. Raymond, J.L. Azanza, Proteasome and myogenesis, Mol. Biol. Rep. 24 (1997) 77–81.
[44] S.C. Boutet, M.H. Disatnik, L.S. Chan, K. Iori, T.A. Rando, Regulation of Pax3 by proteasomal degradation of monoubiquitinated protein in skeletal muscle progenitors, Cell 130 (2007) 349–362.
[45] L. Sun, J.S. Trausch-Azar, A. Ciechanover, A.L. Schwartz, Ubiquitin-proteasome-mediated degradation, intracellular localization, and protein synthesis of MyoD and Id1 during muscle differentiation, J. Biol. Chem. 280 (2005) 26448–26456.
[46] E.M. Creagh, B.M. Murphy, P.J. Duriez, C.S. Duckett, S.J. Martin, Smac/Diablo antagonizes ubiquitin ligase activity of inhibitor of apoptosis proteins, J. Biol. Chem. 279 (2004) 26906–26914.
[47] H.C. Dan, M. Sun, S. Kaneko, R.I. Feldman, S.V. Nicosia, H.G. Wang, B.K. Tsang, J.Q. Cheng, Akt phosphorylation and stabilization of X-linked inhibitor of apoptosis protein (XIAP), J. Biol. Chem. 279 (2004) 5405–5412.
[48] J.C. Jeong, M.S. Kim, T.H. Kim, Y.K. Kim, Kaempferol induces cell death through ERK and Akt-dependent down-regulation of XIAP and survivin in human glioma cells, Neurochem. Res. 34 (2009) 991–1001.
[49] J. Wang, W. Zhang, Y. Zhang, Y. Chen, B. Zou, B. Jiang, R. Pang, Q. Gu, L. Qiao, H. Lan, H.F. Kung, B.C. Wong, c-Jun N-terminal kinase (JNK1) upregulates XIAP-associated factor 1 (XAF1) through interferon regulatory factor 1 (IRF-1) in gastrointestinal cancer, Carcinogenesis 30 (2009) 222–229.
[50] E.M. McMillan, J. Quadrilatero, Autophagy is required and protects against apoptosis during myoblast differentiation, Biochem. J. 462 (2014) 267–277.
[51] Y. Suzuki, Y. Nakabayashi, K. Nakata, J.C. Reed, R. Takahashi, X-linked inhibitor of apoptosis protein (XIAP) inhibits caspase-3 and -7 in distinct modes, J. Biol. Chem. 276 (2001) 27058–27063.
[52] Y. Morizane, R. Honda, K. Fukami, H. Yasuda, X-linked inhibitor of apoptosis functions as ubiquitin ligase toward mature caspase-9 and cytosolic Smac/DIABLO, J. Biochem. 137 (2005) 125–132.
[53] M. MacFarlane, W. Merrison, S.B. Bratton, G.M. Cohen, Proteasome-mediated degradation of Smac during apoptosis: XIAP promotes Smac ubiquitination in vitro, J. Biol. Chem. 277 (2002) 36611–36616.
[54] L.C. Hunt, A. Upadhyay, J.A. Jazayeri, E.M. Tudor, J.D. White, Caspase-3, myogenic transcription factors and cell cycle inhibitors are regulated by leukemia inhibitory factor to mediate inhibition of myogenic differentiation, Skelet. Muscle 1 (2011) (17-5040-1-17).
[55] C. Sun, M. Cai, A.H. Gunasekera, R.P. Meadows, H. Wang, J. Chen, H. Zhang, W. Wu, N. Xu, S.C. Ng, S.W. Fesik, NMR structure and mutagenesis of the inhibitor-of-apoptosis protein XIAP, Nature 401 (1999) 818–822.
[56] S.B. Bratton, J. Lewis, M. Butterworth, C.S. Duckett, G.M. Cohen, XIAP inhibition of caspase-3 preserves its association with the Apaf-1 apoptosome and prevents CD95- and Bax-induced apoptosis, Cell Death Differ. 9 (2002) 881–892.